Changes of the geometry and band structure of SiC along the orthorhombic high-pressure transition path between the zinc-blende and rocksalt structures

M. S. Miao, Margarita Prikhodko, and Walter R. L. Lambrecht
Department of Physics, Case Western Reserve University, Cleveland, Ohio 44106-7079
(Received 6 May 2002; published 15 August 2002)

Using the first principles pseudopotential plane-wave method and the full-potential linearized muffin-tin orbital method, we study how the geometry and the electronic structures change along the orthorhombic transition paths of zinc blende (ZB) to rocksalt (RS) under high pressure. Two different paths, called the fixed strain (force-free) path and the fixed position (hydrostatic stress) path, pass both through the same transition state at any pressure. The actual transition point, however, depends on pressure. The force free path shows a turning point where the atoms jump to the RS positions. A stronger response to changes in either the intersublattice displacement or the strain is observed near the transition state than near the end phases. A phenomenological model helps to reveal that the transition state (TS) is the result of the long-range periodic dependence of the energy on the order parameter whereas the turning point is the result of the local dependence around RS. The band structures show that the TS is metallic although both ZB and RS are semiconductors. This explains the softening of the optical phonons under large strains and why the energy barrier for the relative movements of the sublattices is very low when the strains are kept at the TS.

DOI: 10.1103/PhysRevB.66.064107 PACS number(s): 61.50.Ah, 61.50.Ks, 81.30.Hd

I. INTRODUCTION

Density-functional (DFT) calculations have played an important role in the study of high-pressure phase structures and transition pressures. Recently[1–7] it has become possible to also study the transition path that connects the original and final states via the changes of the unit cell and the displacement of the atoms within the cell. These works vary from the simple tetragonal Bain paths[1] for the bcc to fcc transitions for metals to the more complex paths applicable to the wurtzite and zinc blende to rocksalt transitions[5–7] for some semiconductors. Continuous path studies assume a cooperative movement of the atoms that keeps the translational symmetry and thus neglect the effects of impurities and dislocations. The fact that there is a large hysteresis cycle and that it is greater in pure or thermally treated crystals and especially in the first hysteresis cycle[8] reveals the existence of a large activation energy, which indicates the cooperative movement of the atoms during the transition.

The transition from the zinc blende (ZB) structure to the rocksalt (RS) structure is very common for ionic semiconductors at high pressure. As stated in Ref. 9, group-IV and -III-V semiconductors usually undergo a transition from ZB to β-Sn structure. But x-ray-diffraction investigations of SiC at high pressure[10,11] indicate a ZB to RS transition at a pressure above 100 GPa. This is in fact consistent with the high ionicity of SiC in spite of being a IV-IV compound which arises from the unusual behavior of the energy levels of the second row of the Periodic Table.[12] Recently, a path with an orthorhombic intermediate state has been revealed by a molecular-dynamics[13] simulation for silicon carbide (SiC), and further studied in more detail by least-enthalpy calculations employing a periodic linear combination of atomic orbitals method in conjunction with the density-lowest-combinations of atomic orbitals functional method.[7]

The problem that complicates these phase transitions is that the path might not be unique and the system can transform from one phase to the other by passing through various closely related paths. A recent work[1] showed that metal epitaxial films undergo a bcc to fcc transformation through various Bain paths, and how it can be controlled by the external conditions. While an isotropic stress or strain is imposed in the (001) plane accompanied by vanishing stress perpendicular to the plane, the transition goes through the epitaxial Bain path.[1] On the other hand, if the stress is uniaxial along the [001] axis accompanied by zero stress in the (001) plane, the path is called the uniaxial Bain path.[14]

In a recent comment[15] on Ref. 7, we pointed out that for a transition with the relaxation of both the unit cell and the internal coordinates, the path could vary even if the external condition is fixed by a macroscopic hydrostatic pressure. The path that was studied in Ref. 7 chose fixed atomic positions and allowed lattice vectors to relax. A path with a chosen imposed strain and relaxed atomic positions was proposed in our comment.[15] Both of these paths pass through the same transition state (TS) at which the barrier height is maximum. A further study of the position of the TS, how it is changed with the external pressure and on which structure factors it depends, is of interest. Besides these, how the geometry and the electronic structure change when the system goes through the transition paths, especially around the TS, is also important for understanding the mechanism of the transition. On the other hand, it is not possible to choose the favored path solely by comparing their enthalpies along the path. To confirm the strain driven mechanism proposed in our comment,[15] we need to study the whole landscape of the enthalpy in the relevant parameter space.

In this paper, we present computational results for SiC on the transition paths from ZB to RS under various external pressures, including the position and the properties of the transition state. The changes of the geometry and the electronic structures along the paths are also presented. To gain further insight, a phenomenological model is developed that

mimics the behavior of the first-principles computational results. The analytic solutions of this model provide important insights into various aspects of the transition. The optimum choice among the paths described is discussed on the basis of the enthalpy landscape.

The presentation is organized as follows. The computational methods used will first be briefly introduced in Sec. II. In the presentation of the results (Sec. III), we first (Sec. III A) show the enthalpy curves versus both z and a and point out that the choice of the path cannot be determined solely by their enthalpy comparison. Then the enthalpy landscapes in the whole z and a parameter space are presented for three different pressures: 0 GPa, 63 GPa and 93 GPa. The paths in $z-a$ space are marked and the positions of TS are shown. In Sec. III B the force and the stress equilibrium conditions are described in detail with the help of a phenomenological model that displays the periodic dependence of the energy on z. The model is also used to discuss the changes of the geometry and the properties of the TS point. Some further details on the model are described in Appendixes A and B. Finally, in Sec. III C the electronic densities of states along the path and the band structures for ZB, RS, and the TS are presented and their significance for the transition mechanism is discussed. The conclusions are summarized in Sec. IV.

II. COMPUTATIONAL METHOD

The structural optimization in this article is based on a modified variable-cell-shape[16] dynamics which changes the positions of the ions and the components of the metric (the dot products between the lattice vectors of the simulation cell). Troulliers-Martins pseudopotentials[17] and the plane-wave basis are used. The core radii are 2.50 Å for Si s and p orbitals and 1.50 and 1.54 Å for C s and p orbitals. Test calculations revealed that an adequate cutoff energy for the plane waves is 60 Ry, and a **k**-mesh of $4\times4\times4$ is found to be sufficient for the ZB, RS, and the intermediate structures. The total energy was converged to 5 meV with the above parameters. The Perdew-Wang[18] generalized gradient approximation (GGA) is used for the exchange and correlation potential and energy. The electronic structures are studied by a full potential linear muffin-tin orbital (FP-LMTO) method.[19] So-called smooth Hankel functions[20] are used as envelope functions instead of ordinary Hankel functions. This allows for a smaller basis set to be used. A uniform mesh in real space is used to describe the smooth part of the wave functions, the charge density, and the potential in the interstitial region. This procedure avoids empty spheres completely, which is important here to enable us to treat the structures under continuous transformation in which the interstitial region drastically changes shape and fractional volume of the total volume.

III. RESULTS AND DISCUSSIONS

A. Changes of geometry along the path

The Zb and RS structures are cubic with the space groups of $F\bar{4}3m$ and $Fm\bar{3}m$, respectively. The space group of the intermediate structure that connects the ZB and RS is the subgroup of $F\bar{4}3m$ and $Fm\bar{3}m$, and was determined as $Pmm2$ in Ref. 7. The associated unit cell is chosen as $\mathbf{a}=a(1/2,1/2,0)$, $\mathbf{b}=a(-1/2,1/2,0)$, and $\mathbf{c}=a(0,0,1)$ with respect to the conventional cubic axes and in terms of the cubic lattice parameter a (see Fig. 1). Placing the Si atoms at the origin and at $a(0,1/2,1/2)$ and the C atoms at $a(1/4,1/4,1/4)$ and $a(-1/4,1/4,3/4)$, the path consists of changing the z coordinates of the C atoms from 1/4 to 1/2 and 3/4 to 1. In practice ten equal steps were chosen. At each step, the lattice vectors were relaxed by a variation of the enthalpy, while maintaining the orthorhombic symmetry but allowing one to break the original tetragonal symmetry, until identical stress is obtained for all three directions of the orthorhombic cell. But, as shown in our comment,[15] the intermediate structure is actually body-centered-othorhombic and the corresponding space group is Im$m2$. The volume V and the c/b and a/b ratios (or equivalently a,b, and c) are the free lattice parameters, and z is the only free parameter of the atom position.

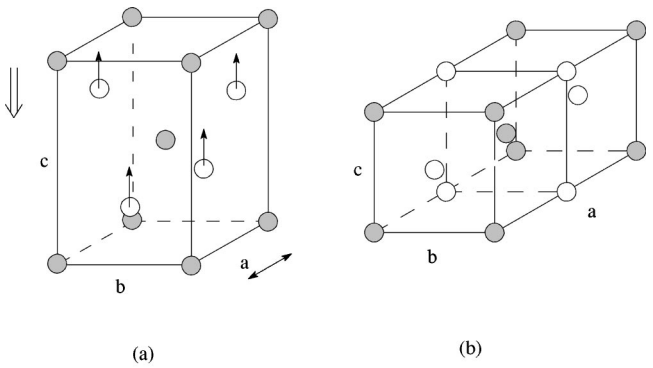

FIG. 1. Unit cell used for the calculations shown in the two end structures (a) ZB and (b) RS.

For the transition path, we first follow Ref. 1 and optimize the enthalpy versus the lattice vectors at each fixed carbon position along the path. The calculation is performed at the calculated transition pressure of 63 GPa. We define this path as a fixed position path (FPP). A barrier of 0.73 eV is obtained at $z=0.34$. The changes of the lattice constants versus z are found to be in good agreement with those of Ref. 1. Next we fully relax the atom positions with lattice constants fixed at the previous optimized values. We will call this path the fixed strain path (FSP). Figure 2(a) shows how the enthalpy changes with the a lattice parameter (and hence strain) for the FPP and FSP. The barrier height has not been changed since both paths pass through the same saddle point, but the enthalpy difference at any given point along the different paths can be as large as 0.25 eV. This does not indicate that the FSP is favored energetically over FPP because the comparison is made at the same strain. If enthalpies for the two paths are compared for the same z value then the curve of the relaxed path lies above that of the unrelaxed one [see Fig. 2(b)]. Thus the enthalpy comparison along the path does not tell us which one is more favored.

In principle, to study the geometry of the FSP, one should perform calculations with one fixed lattice constant and fully relax the other two and the atom position. This requires a constraint optimization. To test the validity of keeping the

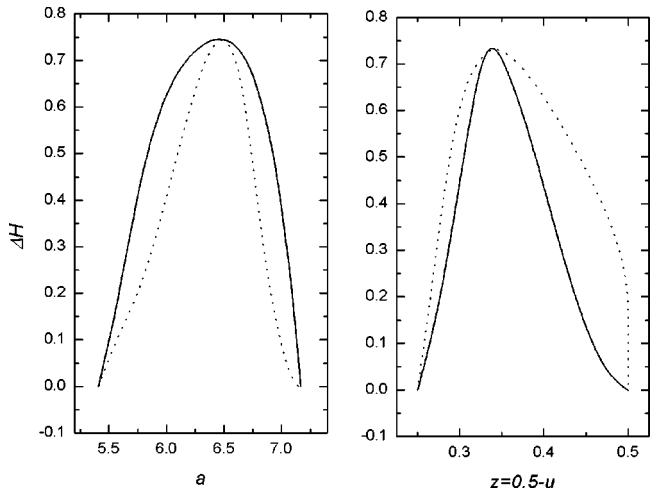

FIG. 2. Enthalpy vs a and z for both the fixed strain path (FSP) (solid line) and fixed position path (FPP) (dotted line) at the transition pressure.

lattice constants of the FSP the same as the values of the FPP, we perform a full optimization for all the lattice constants and atom position at the transition pressure, but at each step set the value of a back to its original value. By testing several original geometries and using a smaller step size, we obtain the relaxed b and c that are very close to those of the FPP. We show the results in Fig. 3. The values of a for the sample points are 5.5,5.8,6.2,6.4,6.8, and 7.0. These are different from the values of the sample points for the FPP. This shows that the relaxed b and c are very close to those of the FPP so that it is a good approximation to assume that the lattice always responds in the same way as in the FPP.

The saddle point remains the same for the FSP and the FPP. The corresponding state is usually called the transition state (TS). This point is a minimum as a function of strain and as a function of the the atom position z. But it is a maximum along the direction of the path. The paths that do not pass through the TS should also be considered but they usually correspond to high energy. Of course, in reality, the system can go through any path but with a probability weighted by a Boltzman factor for the corresponding energy.

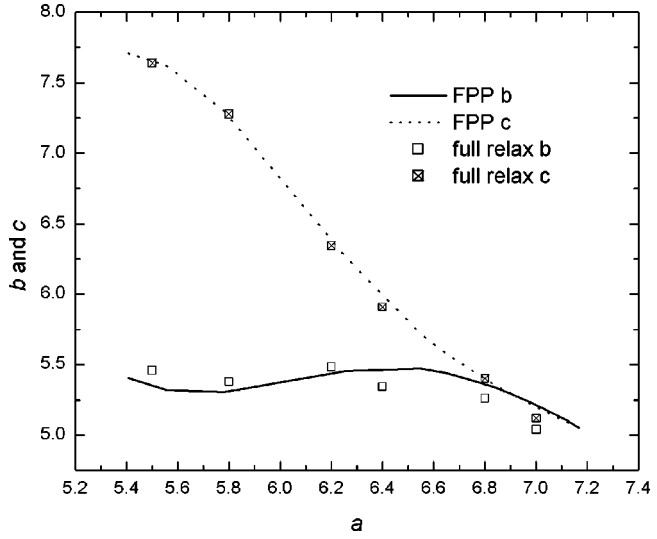

FIG. 3. b and c vs a for FPP and full relaxation. The smooth solid and dotted curves are splined curves for FPP and the open and the crossed squares are points for full relaxation.

Figure 4 shows the total enthalpy as a contour plot as a function of z and a. The FSP and FPP are also plotted in the figure. It should be noticed that for the parameter space with any values of z and a, b and c are kept as those in the FPP path. It is a good approximation around both the FPP and FSP paths (see Fig. 3). A large deviation will occur for the region far away from the above two paths, but those regions are not interesting anyway. One might define an optimum path by the condition of the lowest slope of the enthalpy. Neither the FSP or FPP correspond to this optimum path. Instead, the FSP is a path such that H is at its minimum as a function of the atom position, and the FPP is such that H is at a minimum as a function of the strains. The ideal path with least slope should be in between the FSP and the FPP. At a region close to ZB, it is close to the FSP because the enthalpy derivative versus z is much larger than that versus a, b, and c. It can be seen in Fig. 4 that the contour lines are more dense in the z direction than in the a direction, indicating that the enthalpy increases faster in that direction. Of course, to interpret the spacing of the contours the scales of the two directions must match. If the lattice is kept fixed, the change of z from 0.25 to 0.5 corresponds to the atom movement by $0.25c$, whereas the change of a corresponds to $[1-(1/\sqrt{2})]c$ or about $0.3c$. The corresponding ratio is about the same as shown in Fig. 4. The preference for strain over atomic position changes near the ZB minimum is also consistent with the fact that acoustic phonons have lower energy than the optic phonons around the center of the Brillouin zone.

The basic difference between relaxed and fixed position paths is whether the strain is the driving factor and the motion of the atoms is barely a response to it, or conversely the atom movement is the driving factor and the strains respond accordingly. As we argued, the strain corresponds to the acoustic phonons around the center of the Brillouin zone, whereas the relative movements of the atom correspond to the optic phonons. The former have a much smaller excitation energy. The long-range fluctuations and the local deformations can also cause the required strain and the locally non-hydrostatic stress.

Figure. 4 clearly shows that the FSP and FPP paths have three common points, the ZB, the RS, and the TS. Interestingly, in the region with $a<6.25$, z changes only slightly from its ideal position for the ZB structure, and, in the region $a>6.75$, z jumps to the ideal value of 0.5 for the RS structure. Only in the small region in between do the atom positions change quickly. The slight changes of the atom position around ZB and RS can be viewed as the response intersublattice displacement z to the deformation of the lattice vectors from the ideal ZB and RS structures. It is worth to noticing that the changes of the lattice breaks the tetrahedral symmetry of ZB and the original atom positions are no longer determined by symmetry, i.e., free to move in the z direction. But for RS, although the octahedral symmetry is

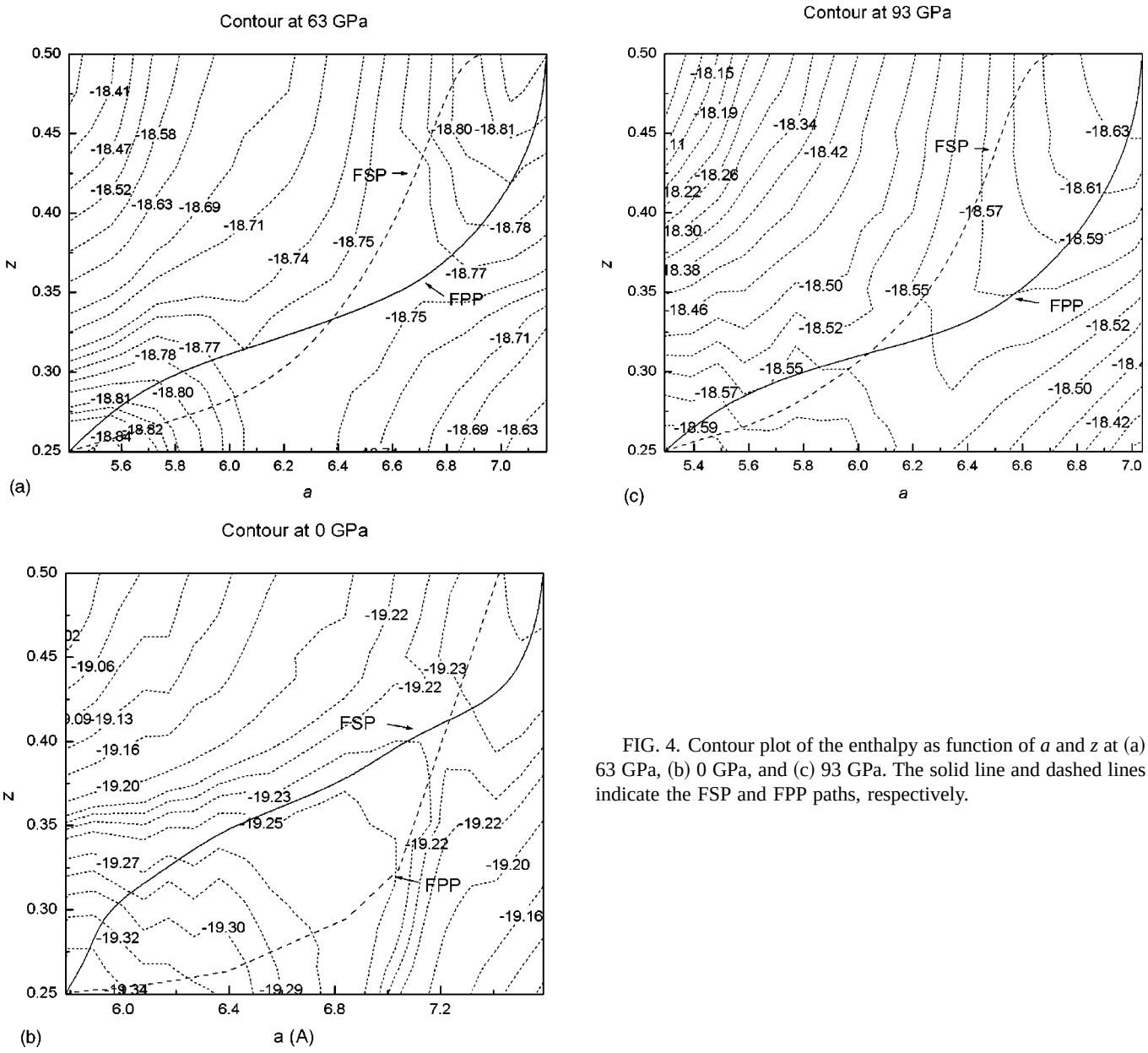

FIG. 4. Contour plot of the enthalpy as function of a and z at (a) 63 GPa, (b) 0 GPa, and (c) 93 GPa. The solid line and dashed lines indicate the FSP and FPP paths, respectively.

broken, the atoms maintain their high-symmetry positions. Because of that, the atoms remain unchanged for fairly large lattice deformations in the RS structure. A similar behavior was also found for the lattice constants in the FPP. That is, when the atomic position is slightly changed from the ZB or RS positions, the lattice parameters at first do not change appreciably. Inspection of the Figs. 4(b) and 4(c) shows that while the pressure increases, the ''resistance towards change'' of the RS structure becomes stronger while that of the ZB becomes weaker. Correspondingly the transition point moves closer and closer to the ZB side.

A similar resistance against change can also be seen in Fig. 5, which shows the dependence of the c/b ratio on the a/b ratio. Interestingly, this resistance is very weak under zero external pressure. The c/b ratio changes with the a/b ratio almost linearly. With increasing pressure, the curves become more s shaped, indicating that c/b can maintain its value over some range of a/b values. Apparently, the RS structure is more resistant to a change in shape than the ZB structure. For small strains, the response of c/b to a/b is closely related to the Poisson ratio for these particular directions. Apparently, this Poisson ratio depends on pressure.

Figure 6 shows the energy dependence on the atom positions while the strains or lattice constants are those for the ZB, RS, and TS states at the transition pressure. By ZB and strains, here we mean the strains of the orthorhombic unit cell which lead to the ZB and RS structures if the atoms are relaxed. Here we wish to study the energy of these strained unit cells for any position of the two sublattices in it. Note that this means that the volume is different for each curve but stays constant along the curve. Only the right panel corresponds to the region in which the transition occurs between ZB and RS, but the left part is important to derive a complete model for the energy behavior as a function of z. As expected, the curves are periodic. The periodicity for the ''ZB strain'' is half of that for the ''RS strain.'' Since the energy

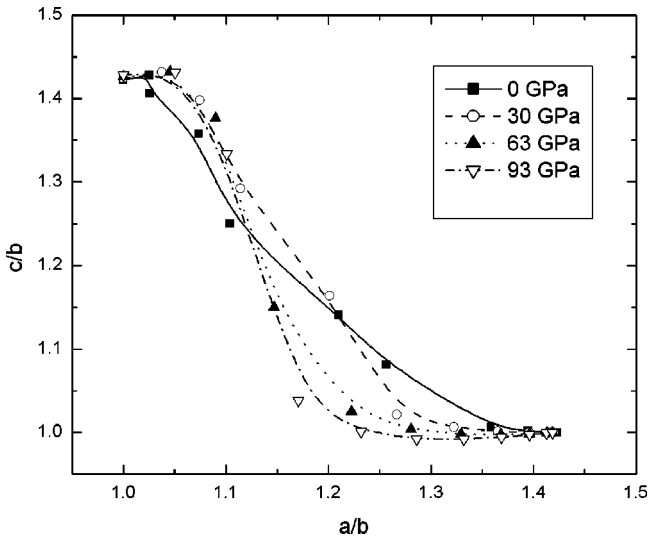

FIG. 5. c/b ratio vs a/b ratio under various external pressures.

rather than the enthalpy is depicted here, there is a difference between the ZB and RS states at their respective minima. If we were to switch to enthalpy, there would simply be a shift of the whole curve by a constant such that now the minima of the curves line up.

Interestingly, the ZB curve fits very well to a cosine function with a period of 0.5. The deviation is so small that it can hardly be seen in Fig. 6. On the other hand, there is a larger difference between the RS curve and the cosine function which has the same height and periodicity. The difference is more obvious when the system moves to the ZB positions. The real RS curve is lower than the ideal cosine curve. In the following, we will first neglect this difference and set up a phenomenological model based on a linear combination of the two cosine functions that define the periodic behavior of the total energies as function of z for unit cells corresponding to the ZB and RS strains, respectively. Later on, we will discuss the effect of the above omission.

The TS curve is very flat in the right panel, indicating that the relative movements of the two sublattices becomes much easier while the strains are imposed to form the TS lattice. In other words, the optical phonon is strongly softened while the strains along the FSP path are imposed. Combining this with the strain-driven mechanism at the beginning of the path, we now obtain the whole picture of the transition procedure. The transition is induced by lattice fluctuations that become softer under high pressure. The atoms move accordingly in response but with a large resistance. When large strains are imposed, however, the optical phonon becomes strongly softened and the atoms pass over the TS position and go quickly to the RS position. This will further cause the relaxation of the lattice toward its RS form.

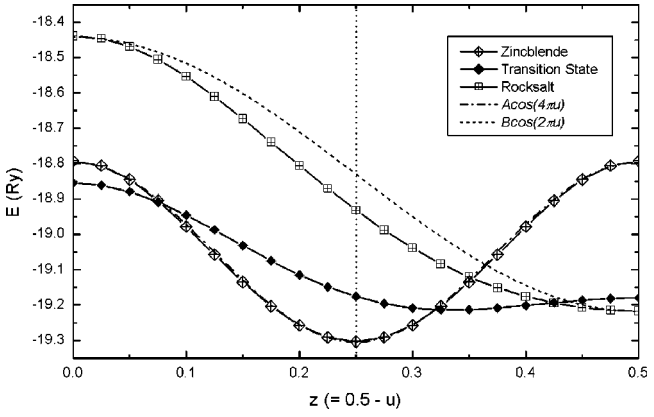

FIG. 6. The total energy versus z for strains of the orthorhombic cell corresponding to ZB, RS, and TS lattices. The short dashed and dotted lines are the fitted cosine functions.

B. Equilibrium conditions and the transition state

The TS curve in Fig. 6 is representative of all the intermediate states between the ZB and RS structures. Approximately, the TS curve is the superposition of the ZB and RS curves, plus an additional down shift caused by the lattice relaxation. Inspired by this observation, we assume that the enthalpy for the points in between the two extreme structures will just be a linear combination of those two with coefficients which depend linearly on the strain. In this way, we introduce the coupling between the strains and the internal parameter u. After adding the elastic contribution in a quadratic form, we obtain a model enthalpy of the form

$$\Delta H = \frac{1}{2}\eta^{\mathrm{T}}\mathbf{C}\eta + A\eta^{\mathrm{T}}\xi\cos 4\pi u + B(\eta^{\mathrm{T}}\xi - \eta_Z^{\mathrm{T}}\xi)\cos 2\pi u - (A+B)\eta^{\mathrm{T}}\xi, \quad (1)$$

in which $\eta^{\mathrm{T}}=(\eta_1\eta_2\eta_3)$ is the strain vector that contains only the diagonal elements of the strain tensor (because we maintain orthorhombic symmetry such that the orthorhombic axes are the principal axes of the strain tensor); $\mathbf{C}$ is the elastic constant matrix in Voigt notation, appropriate for this choice of axes; and $\xi^{\mathrm{T}}=(\alpha\beta\gamma)$ is the coupling coefficient between u and the strains. It is also assumed that $\eta=\mathbf{0}$, while the system is in the RS structure and $\eta=\eta_{\mathrm{ZB}}$ while in the ZB structure. While Fig. 6 displayed energies, here we return to enthalpies at the transition pressure. Thus the elastic constants and the strains η are defined with respect to the RS enthalpy and lattice parameters.

The first-order derivatives versus the strains give the total stress in the three directions of the orthorhombic cell and the derivative versus u gives the force on the atoms. At equilibrium, both stresses and forces should be zero:

$$\frac{\partial H}{\partial \eta^{\mathrm{T}}} = \mathbf{C}\eta + A\xi\cos 4\pi u + B\xi\cos 2\pi u - (A+B)\xi = \mathbf{0}, \quad (2)$$

$$\frac{\partial H}{\partial u} = -4\pi A\eta^{\mathrm{T}}\xi\sin 4\pi u - 2\pi B(\eta^{\mathrm{T}}\xi - \eta_Z^{\mathrm{T}}\xi)\sin 2\pi u = \mathbf{0}.$$

Usually, the two equilibrium conditions cannot be satisfied simultaneously. In the whole parameter space, only three points can have both zero stress and zero force. They are the initial ZB, the final RS, and the TS. These three states are minima for both strains and u, but the ZB and RS are minima

in all directions while the transition state is a saddle point because it exhibits a maximum along the direction of the path. Along the FPP, the stress is zero but large forces remain on the atoms. On the other hand, for the FSP, the forces are zero but stresses exist and are generally unequal along the three directions. The trace of the stress matrix divided by three gives the deviation from the transition pressure, which will be assumed to stay zero, so that the stress matrix must remain traceless. However, as long as it has nonzero components there is a deviation from hydrostatic stress. As discussed in Sec. III A, both paths pass through TS point.

The parameters, A,B, and ξ can be determined by fitting the results of the model to the calculated values of ZB and TS states. But, as we will show in the following, the absolute values of these parameters are irrelevant to the position of the TS as well as that of the turning point. In the RS state $u=0$ and $\eta=0$, and thus the equilibrium condition is obviously satisfied. In the ZB state, $u=1/4$. From the first condition, one obtains

$$\mathbf{C}\,\eta_Z=(2A+B)\xi. \tag{3}$$

As shown in Appendix A, the condition of having equal enthalpies for ZB and RS at the transition pressure leads to $\mathbf{C}\,\eta_Z=4A\xi$. Combining this with the above equation gives $B=2A$. This is approximately true for the energy potential curves in Fig. 6.

The TS can be obtained by generally solving Eq. (2). The resultant equation for the TS is

$$\cos 2\pi u=-\frac{3}{8}\frac{B}{A}+\frac{1}{8}\sqrt{\left(\frac{B}{A}\right)^2+32\frac{B}{A}+64}. \tag{4}$$

This indicates that the position of the transition state depends only on the B/A ratio at the transition pressure. If $B/A=2$, then $\cos 2\pi u=0.686$ and $u=0.13$. It is interesting that the position of the TS depends only on the B/A ratio but not on the elastic properties of the lattice. This is the result of the linear coupling and the harmonic approximation. It reveals that the position of the TS is defined mainly by the symmetry. The effects of the deviation of the RS curve from a cosine function in Fig. 6 can be seen from their crossing with the ZB curve. Since the enthalpy for a general value of the strain is a linear combination of the ZB and RS strain enthalpies, the TS, which by definition corresponds to the highest enthalpy along the path as function of u, must be near the crossing point. One can see that using the ideal cosine function moves the crossing point and the TS toward the RS. This is consistent with the fact that the model gives a TS closer to RS than the first-principles calculation gives.

Next we consider the effects of pressure deviating from the transition pressure. Generally, the enthalpy difference between the ZB and RS structures (i.e., both strains and u values corresponding to ZB and RS) can be related to the A and B parameters as follows:

$$\Delta H=\frac{B-2A}{2}\,\eta_Z^{\mathrm{T}}\xi, \tag{5}$$

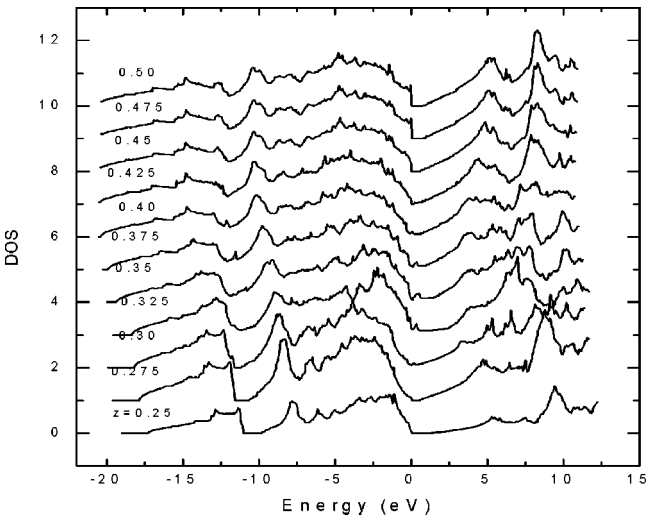

FIG. 7. Density of states along the FPP.

in which $\Delta H=H_{ZB}-H_{RS}$. Details are given in Appendix A. At a pressure higher than the transition pressure, $\Delta H>0$, so $B/A>2$. This will reduce the value of $\cos 2\pi u$ in Eq. (4) as $\cos 2\pi u$ depends on B/A almost linearly with a negative slope. The result is a larger u or smaller z, which explains that the TS moves toward ZB at a pressure higher than the transition pressure. The increase of the B/A ratio is also confirmed by the calculations.

The turning point, i.e., the point at which the system jumps to the ideal u for the RS structure along the fixed-strain path, is different from the TS point. Here instead of satisfying both the stress and force equilibrium conditions, the system satisfies the force equilibrium condition $\partial H/\partial u=0$ and the turning point condition $\partial^2 H/\partial u^2=0$ which gives

$$16A\,\eta^T\xi\cos 4\pi u-B(\,\eta^T\xi-\delta)\,\eta^T\xi\cos 2\pi u=0. \tag{6}$$

Combining the above equation with the force equilibrium [Eq. (2)] gives $u=0$ as the only solution which corresponds to the RS structure. Thus in this model there is no turning point. However, a slight modification of the model will lead to a turning point at a strain value slightly before the RS phase is attained, as discussed in Appendix B.

C. Electronic structure in transition

As shown in Fig. 6, the energy barrier becomes very shallow while the strains are kept the same as those for the TS. This indicates that the bonds are significantly softened. It is therefore interesting to investigate how the electronic structure changes along the path. For this purpose, we perform band-structure calculations using the FP-LMTO method for the states along the transition paths. The geometries are adopted from the pseudopotential calculations at the transition pressure. Figure 7 shows the density of states (DOS) at different points along the FPP. The two DOS's with $z=0.25$ and 0.5 correspond to the ZB and the RS structures, respectively. Because the RS structure is more dense than the ZB structure, the valence bands are widened for RS. The gap at around -10 eV for ZB separates the two subgroups of

the valence bands. The lower group comprises mostly C *s* bonding states with Si *s* and Si *p* orbitals whereas the upper subgroup are mostly composed of C *p* bonding with Si *s* and Si *p* orbitals. In the ZB structure they are very well separated because of the breaking of the inversion symmetry. While changing to RS structure, this gap gradually decreases and closes around the TS state. The fundamental gap between the valence and conduction bands exists for both ZB and RS structures, indicating that both structures are semiconductors. Interestingly, this gap closes around the TS state, indicating that the TS is metallic. Although the gap closes, there remains a dip structure. So the TS can be identified as a ''poor'' metal. The DOS changes along the FSP are similar, since it goes through the same TS state as the FPP.

To see what happened to the gap, we show the FP-LMTO band structure for ZB, TS, and RS structures in Fig. 8. For comparison, all three cases are shown in a simple orthorhombic Brillouin zone. The notation of the symmetry points follows Bradley and Cracknell.[21] It can be seen that at the transition pressure, the ZB and RS are still semiconductors with (GGA) band gaps of 1.5 and 0.75 eV, respectively. But the TS is metallic with a band overlap of more than 2 eV. Note that the ZB band gap here appears to be direct, while ZB SiC is well known to have an indirect gap at *X*. This is because the *X* minimum of the ZB structure has been folded to the Γ point in the present orthorhombic Brillouin zone (BZ). The major change in the TS is the band overlap. Also the triplet degeneracy of the valence band maximum is broken by the symmetry breaking. Although the local density approximation (LDA) or the GGA has a tendency to underestimate the band gaps, this large overlap rules out the possibility of being an artifact of the GGA. The band overlap happens merely around the Γ point. The rest of the band structure still has a close resemblance to the bands in the ZB and RS structures.

IV. CONCLUSIONS

In conclusion, we have investigated the changes of the geometry and electronic structures of SiC along the transition paths from ZB to RS using both the pseudopotential plane-wave and FP-LMTO methods. Although there are various nonequivalent paths to consider, the most adequate paths should pass through the transition state. The TS state corresponds to both a force and stress equilibrium. The fixed strain path (FSP) corresponds to a force equilibrium only and the fixed position path (FPP) corresponds to a stress equilibrium. These equilibrium conditions are satisfied throughout the paths. Besides the TS, there is a turning point for the FSP at which the atoms jump to their ideal RS positions. Both paths show a strong resistance against deviation from the ideal ZB and RS structures when small perturbations from the latter are considered. When the pressure increases, the TS state moves toward ZB. A phenomenological model is proposed, in which the strains and the periodic function of the internal structural parameter are coupled. The TS is found to be the result of the long-range periodic structure, whereas the turning point is the result of the nonlinear dependence around the RS structure. The band structure reveals that the system is metallic around the TS, which explains the softening of the bonds in that state.

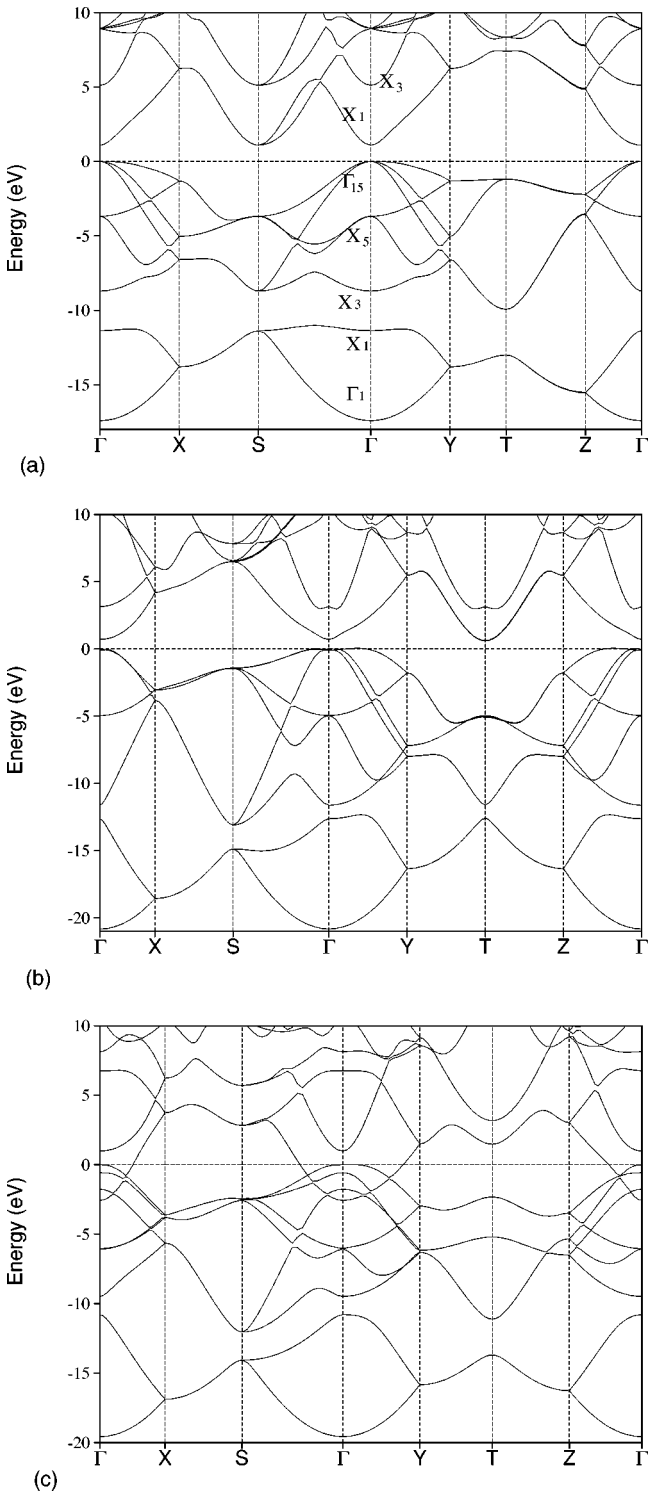

FIG. 8. The LDA band structure for (a) ZB, (b) RS, and (c) TS in a common orthorhombic Brillouin zone. The labels for the ZB case correspond to the ZB BZ.

Although the system can go through many paths connecting ZB and RS structures, it favors the paths close to FSP, which is consistent with the fact that the fluctuation of the strains requires less energy than the fluctuation of the atom

positions. While large strains are achieved, the optical phonon is significantly softened and the atoms can easily move from the ZB- to RS-type internal position. After it goes through the TS state, the atom quickly moves toward its RS position and causes a further relaxation of the lattices.

ACKNOWLEDGMENT

This work was supported by the ONR under Grant No. N000-99-1-1073.

APPENDIX A: THE MODEL IN THE RS AND ZB LIMITS

In the RS limit, $u=0, \eta=\mathbf{0}$,

$$H_{RS}=-B\,\eta_Z^{\mathrm{T}}\xi, \tag{A1}$$

while in the ZB limit $u=1/4, \eta=\eta_Z$ and

$$H_{ZB}=\frac{1}{2}\,\eta_Z^{\mathrm{T}}\mathbf{C}\,\eta_Z-A\,\eta_Z^{\mathrm{T}}\xi-(A+B)\,\eta_Z^{\mathrm{T}}\xi. \tag{A2}$$

At the transition pressure, $H_{ZB}=H_{RS}$. So that

$$\eta_Z^{\mathrm{T}}\mathbf{C}\,\eta_Z=4A\,\eta_Z^{\mathrm{T}}\xi. \tag{A3}$$

If the strains are kept as those of RS, i.e., $\eta=\mathbf{0}$ then H is a function of u only:

$$H=-B\,\eta_Z^{\mathrm{T}}\xi\cos 2\pi u. \tag{A4}$$

Otherwise, if the strains are kept as those for ZB, i.e., $\eta=\eta_Z$, then

$$H=\frac{1}{2}\,\eta_Z^{\mathrm{T}}\mathbf{C}\,\eta_Z+A\,\eta_Z^{\mathrm{T}}\xi\cos 4\pi u-(A+B)\,\eta_Z^{\mathrm{T}}\xi. \tag{A5}$$

On the other hand, if the atoms are kept at their ideal RS positions, i.e., $u=0$, the enthalpy depends only on the strains:

$$H=\frac{1}{2}\,\eta^{\mathrm{T}}\mathbf{C}\,\eta-B\,\eta_Z^{\mathrm{T}}\xi. \tag{A6}$$

Or if $u=1/4$, the atoms are in their ZB positions, then

$$H=\frac{1}{2}\,\eta^{\mathrm{T}}\mathbf{C}\,\eta-A\,\eta^{\mathrm{T}}\xi-(A+B)\,\eta^{\mathrm{T}}\xi. \tag{A7}$$

This equation can be rewritten around ZB strains as

$$\begin{aligned}H&=\frac{1}{2}(\eta^{\mathrm{T}}-\eta_Z^{T})\mathbf{C}(\eta-\eta_Z)+\eta^{\mathrm{T}}\mathbf{C}\,\eta_Z\\&\quad-\frac{1}{2}\,\eta_Z^{\mathrm{T}}\mathbf{C}\,\eta_Z-A\,\eta^{\mathrm{T}}\xi-(A+B)\,\eta^{\mathrm{T}}\xi\\&=\frac{1}{2}(\eta^{\mathrm{T}}-\eta_Z^{T})\mathbf{C}(\eta-\eta_Z)-\frac{1}{2}\,\eta_Z^{\mathrm{T}}\mathbf{C}\,\eta_Z.\end{aligned} \tag{A8}$$

The second step is because

$$\eta^{\mathrm{T}}\mathbf{C}\,\eta_Z=A\,\eta^{\mathrm{T}}\xi+(A+B)\,\eta^{\mathrm{T}}\xi \tag{A9}$$

which is the stress equilibrium condition at the ZB point. So now the enthalpy depends on the strains measured from the ZB structure. This shows that within our model the elastic constants of ZB defined as second derivatives versus strain of the enthalpy at fixed position $u=1/4$ are the same as those of RS. The actual elastic constants of ZB should, however, be defined in terms of the ZB enthalpy relaxed versus the internal parameter, and will therefore be lower. In fact, within the model, we obtain the same elastic constants as for RS all along the FPP. This approximation may not correspond exactly to reality, and derives from our use of a model which attempts to describe the ''global'' behavior as a function of u while as function of η it assumes a quadratic expansion around RS and a linear coupling between the two which strictly is only valid for small η. However, it is important to note that the position of the TS and the turning point do not depend on the values of $\mathbf{C}$ nor on the coupling constants ξ. As shown in the main text, it is the result of the long range periodicity and depends only on the A/B ratio.

APPENDIX B: MODIFICATION OF THE ENTHALPY DEPENDENCE AND THE TURNING POINT

In this appendix, it is shown that a turning point, i.e., a point where the structure jumps discontinuously from the ZB to the RS u value before the strain corresponding to the RS phase is achieved. To do this, we modify our model enthalpy to include the effect of the deviation from the cosine function for the ''RS strain'' term. The RS curve in Fig. 6 shows that the energy changes slower than the ideal cosine function, which also indicates a weaker coupling between the strains and the internal parameter. To include this fact, we assume an extra linear coupling term around the RS structure in the model enthalpy with a negative slope,

$$\begin{aligned}H&=\frac{1}{2}\,\eta^{\mathrm{T}}\mathbf{C}\,\eta+A\,\eta^{\mathrm{T}}\xi\cos 4\pi u\\&\quad+B(\eta^{\mathrm{T}}\xi-\eta_Z^{\mathrm{T}}\xi)(\cos 2\pi u-\alpha u)-(A+B)\,\eta^{\mathrm{T}}\xi,\end{aligned} \tag{B1}$$

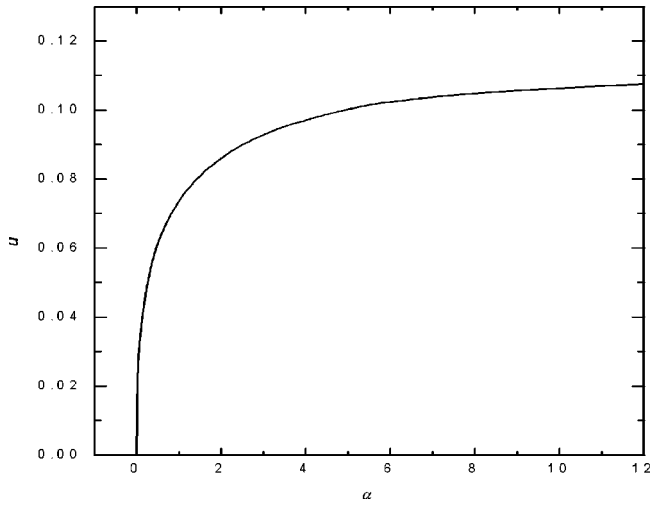

FIG. 9. The turning point position as a function of the linear coupling coefficient α.

in which $\alpha > 0$. This linear coupling term breaks the periodicity and also the mirror symmetry at the RS point. It should only be assumed to be valid in the right panel of Fig. 6. The corresponding stress and force equilibrium conditions are

$$\mathbf{C}\,\eta + A\xi\cos 4\pi u + B\xi\cos 2\pi u - \alpha B\xi u - (A+B)\xi = \mathbf{0} \tag{B2}$$

and

$$-4\pi A\,\eta^{\mathrm{T}}\xi\sin 4\pi u - 2\pi B(\eta^{\mathrm{T}}\xi - \eta_Z^{\mathrm{T}}\xi)\sin 2\pi u - \alpha B(\eta^{\mathrm{T}}\xi - \eta_Z^{\mathrm{T}}\xi) = \mathbf{0}. \tag{B3}$$

The general solution for the TS is very complex. But as we argued in the text, this negative coupling term will move the TS toward the ZB.

The turning point condition is $\partial^2 H/\partial u^2 = 0$ which gives

$$-16\pi^2 A\,\eta^T\xi\cos 4\pi u - 4\pi^2 B(\eta^T\xi - \eta_Z^{\mathrm{T}}\xi)\cos 2\pi u = 0. \tag{B4}$$

Combining it with the force equilibrium condition and after some simplifications, one obtains

$$\alpha\cos 4\pi u - \pi\sin 4\pi u\cos 2\pi u + 2\pi\sin 2\pi u\cos 4\pi u = 0. \tag{B5}$$

The u versus α curve is plotted in Fig. 9. It can be seen that a small value of α can induce a turning point evidently away from the RS structure. But u becomes quickly saturated and can never be larger than 1/8. In conclusion, a linear coupling term not only moves the TS toward the ZB but also explains the origin of the turning point.

[1] P. Alippi, P.M. Marcus, and M. Scheffler, Phys. Rev. Lett. **78**, 3892 (1997).

[2] A. Martín Pendás, V. Luaña, J.M. Recio, M. Flórez, E. Francisco, M.A. Blanco, and L.N. Kantorovich, Phys. Rev. B **49**, 3066 (1994).

[3] C.E. Sims, G.D. Barrera, N.L. Allan, and W.C. Mackrodt, Phys. Rev. B **57**, 11 164 (1998).

[4] M.A. Blanco, J.M. Recio, A. Costales, and R. Pandey, Phys. Rev. B **62**, 10599 (2000).

[5] S. Limpijumnong and W.R. Lambrecht, Phys. Rev. Lett. **86**, 91 (2001).

[6] S. Limpijumnong and W.R. Lambrecht, Phys. Rev. B **63**, 104103 (2001).

[7] M. Catti, Phys. Rev. Lett. **87**, 035504 (2001).

[8] A. Lacam and J. Peyronneau, J. Phys. (Paris) **34**, 1047 (1973).

[9] J.R. Chelikowsky and J.K. Burdett, Phys. Rev. Lett. **56**, 961 (1986).

[10] M. Yoshida, A. Onodera, M. Ueno, K. Takemura, and O. Shimomura, Phys. Rev. B **48**, 10587 (1993).

[11] T. Sekine and T. Kobayashi, Phys. Rev. B **55**, 8034 (1997).

[12] W. R. L. Lambrecht, in *Diamond, SiC, and Nitride Wide Bandgap Semiconductors*, edited by C. H. Carter, Jr., G. Gildenblat, S. Nakamura, and R. J. Nemanich, MRS Symposia Proceedings No. 339 (Materials Research Society, Pittsburgh, 1994), pp. 565-582.

[13] F. Shimojo, I. Ebbsjö, R.K. Kalia, A. Nakano, J.P. Rino, and P. Vashishta, Phys. Rev. Lett. **84**, 3338 (2000).

[14] F. Milstein, H. Fang, and J. Maschall, Philos. Mag. A **70**, 621 (1994).

[15] M. S. Miao, Margarita Prikhodko, and Walter R. L. Lamberecht, Phys. Rev. Lett. **88**, 189601 (2002).

[16] I. Souza and J.L. Martins, Phys. Rev. B **55**, 8733 (1997).

[17] N. Troullier and J.L. Martins, Phys. Rev. B **43**, 1993 (1991).

[18] J.P. Perdew and Y. Wang, Phys. Rev. B **45**, 13244 (1992).

[19] M. Methfessel, M. van Schilfgaarde, and R. A. Casali, in *Electronic Structure and Physical Properties of Solids, the Uses of the LMTO Method*, edited by Hugues Dreyssé, Springer Lecture Notes, Workshop Mont Saint Odille, France, 1998 (Springer, Berlin, 2000), pp. 114-147.

[20] E. Bott, M. Methfessel, W. Krabs, and P.C. Schmidt, J. Math. Phys. **39**, 3393 (1998).

[21] C. J. Bradley and A. P. Cracknell, *The Mathematical Theory of Symmetry in Solids* (Clarendon, Oxford, 1972).